Proceedings of to the 9th Scientific Conference of University of Garmian: Pure science and Technology Applications (SCUG-PSTA-2022). Kalar (46021) / Sulaymaniyah (26-27 Oct.2022) (Special issue for Passer journal of basic and applied sciences) Paper No. 05, 63-79

Malaria Parasite Identification from Red Blood Cell Images Using Transfer Learning Models

Abdalbasit Mohammed Qadir [1]*, Peshraw Ahmed Abdalla [2], Mazen Ismael Ghareeb[1]

[1*] Department of Computer Science, College of Science and Technology, University of Human Development

[2] Department of Computer Science, College of Science, University of Halabja

Abdalbasit.mohammed@uhd.edu.iq; Peshraw.abdalla@uoh.edu.iq; Mazen.ismaeel@uhd.edu.iq

ABSTRACT

Malaria is a dangerous viral disease caused by Plasmodium protozoan parasites that are spread by the bite of an infected female Anopheles mosquito. This pandemic disease's fast and precise identification is essential for effective treatment. The most reliable method for diagnosing malaria is a microscopic examination of a thick and thin blood smear, which looks for the parasite and counts the number of infected cells. The ability to wholly or partially automate the identification of the disease using the information in medical images highlights the critical role that computer-aided diagnosis plays in modern medicine, in which machine learning and deep learning play a critical role. In this study, we have presented an in-depth overview of the techniques and methods used to diagnose the malaria parasite through blood slides automatically. One of the techniques is using transfer learning models to detect the malaria parasite. We have compared the performance of transfer learning models on identifying infected malaria cells by feeding the models a large dataset of uninfected and parasite cell images. The results show that the DensNet models have the edge over the other models, with DenseNet-201 achieving the highest accuracy and F1 score of 0.9339 and 0.9321, respectively. Also, DenseNet-169 outperformed the other models with 0.9594 in precision, and finally, Densenet-121 had the highest recall with 0.9490.

KEYWORDS: Malaria, Blood smear, Machine learning, Deep learning, Tranfer learning.

1 INTRODUCTION

Malaria is a potentially fatal disease that has spread in many parts of the world. The bites of female anopheles mosquitoes spread it, and the red blood cells are where most malaria parasites live. The stained

blood elements, such as parasites, RBCs (Red Blood Cells), and WBCs (White Blood Cells), are separated. The obtained stained elements are then positioned under a red blood cell mask to separate any possible parasites. The World Health Organization states that every year a total number of 300-500 million malaria cases are reported [1]. Any four parasitic species of Plasmodium are responsible for this: malaria, falciparum, vivax, and ovale. In order to diagnose the current state of the disease, Visual microscopic examination evaluation of Giemsa stained blood smears is the most widely used technique[2]. In today's world, in addition to political efforts and biomedical research, recent advances in information technology have played a crucial role in many attempts to combat the disease. In particular, an early malaria diagnosis has been one of the factors that have led to a mortality reduction. Many techniques varying from image analysis software to machine learning algorithms, were utilized by working on microscopic blood slides to detect parasitemia in order to have a better diagnosis performance. New developments in image processing and artificial intelligence for microscopic malaria detection are discussed, and an overview of these methods is provided in this article. We review the numerous methods for automated cell classification described in the literature, including those for image preprocessing, imaging, cell segmentation, parasite detection, feature calculation, and automatic cell classification. This research has compared the Transfer Learning models' performance in detecting malaria parasites, one of the deep learning techniques.

2 LITERATURE REVIEW

There are several methods for diagnosing malaria, such as the cost of a test, specificity, sensitivity of the approach, user skill level, and time per test, which are all significant factors. Furthermore, as a prognostic indicator, it is helpful to count the total amount of infected red blood cells [3]. The collection of digital images of blood smears is usually the first step. This step is highly dependent on the materials and equipment used. The image acquisition section describes the various types of microscopies, blood slides (thin or thick), and staining are described. After the image acquisition, in order to normalize lighting, remove noise, and staining process, in the image acquisition where colour variations are inherent, most systems employ one or more pre-processing approaches. Based on the methods used, the pre-processing section organizes the publications. Usually, the next step is the segmentation (outlining) and detection of the blood cells, and any other objects shown in the blood slide image, including parasites or platelets.

In many articles, cell segmentation is preceded by a set of features computed mathematically to describe the segmented objects and their visual appearance. Giemsa, the most commonly used stain in practice, has been adopted by thin and thick smears. Even though excellent results for malaria parasites are provided by stains such as Leishman, for routine malaria diagnosis, Giemsa remains the best all-around stain. However, its disadvantage is that it is relatively expensive, but the long-term stability and consistency have outweighed this factor [4-6]. There has been much variety in work done in this field. Nonetheless, a

series of essential processing stages may be used as a guideline by the systems that automated cell microscopy often incorporates. As a result, the following subsections will each concentrate on a single element of the processing pipeline. The first phase often involves taking digital pictures of blood smears, which is highly dependent on the tools and supplies used. In the image capture section, many approaches for various types of microscopies, blood slides (thin or thick), and staining are discussed. Most systems use one or more preprocessing techniques after acquiring images to reduce noise and standardize illumination and color variances brought on by the image acquisition and staining processes. The papers are arranged in the preprocessing section according to the techniques used.

The following stage often entails identifying and segmenting (outlining) individual blood cells and other elements, such as parasites or platelets, that may be seen in a blood slide picture. All segmentation techniques used to diagnose microscopic malaria are summarized in the section headed Red blood cell detection and segmentation [5,7-11]. Most systems use one or more preprocessing techniques after picture acquisition to reduce noise and standardize illumination and color variances brought on by the image acquisition and staining processes. The papers are arranged in the preprocessing section according to the techniques used.

The last phase often entails the identification and segmentation (outlining) of specific blood cells as well as any other items that may be seen, such as parasites or platelets in a blood slide picture. All segmentation techniques that have been utilized to diagnose microscopic malaria are summarized in the section, such as Binocolor microscopy, Polarized microscopy, Fluorescent microscopy, Serial block-face scanning electron microscopy (SBFSEM), Image-based cytometer, SightDx digital imaging scanning, Fiber array-based Raman imaging, Multi-spectral and multi-modal microscopy, Scanning electron microscopy (SEM), Quantitative cartridge-scanner system, Quantitative phase imaging (QPI) and Sub-pixel resolving optofluidic microscopy (SROFM) [12- 17].

There are also several approaches when it comes to analyzing images of digital blood slides automatically, which have adopted the preprocessing process and been applied to reduce the variation of unnecessary duplicated images in this process and enhance the quality of the image. Noise removal, staining correction, contrast adjustment, and lighting, are the three main goals. Popular filters like Gaussian low-pass filtering, mean and median filters have historically been the most frequently used methods for noise reduction. Furthermore, using morphologic processes is quite common. The most often used methods for contrast enhancement, in particular, techniques for contrast stretching, histogram equalization, and color normalizing, are utilized for differences in lighting and staining, including the widely used grayscale colors [18-23].

Understanding red blood cell identification and segmentation is crucial. Most of these methods include thresholding, including Otsu thresholding in conjunction with morphologic processes. However,

it's possible that the relative simplicity of these procedures is what makes them so dominant rather than their higher performance when compared to other approaches. Other techniques include unsupervised k-means pixel clustering and the Active Contour, which makes assumptions about the morphology of blood cells.

Appropriate cell segmentation is required for the precise parasitemia to be calculated. However, recognizing and separating the individual cells can be challenging when touching cells. To overcome this problem, many techniques, such as watershed and active contours, are useful [24-30].

Feature extraction and selection, the appearance of uninfected and infected red blood cells in thin smears is described by a variety of characteristics in the literature. Naturally, color aspects are most natural and are, in fact, employed by many articles since parasites have been stained. Additionally, the inside of red blood cells has been described using a variety of morphological and textural characteristics. It is speculated that these qualities may cause infected cells to seem to be normal, even down to the ring structures and the obvious cytoplasm. Most of the features are tried and reliable implementations that have been used in other, sometimes non-medical contexts [8,13,25,31-35].

Almost all classification techniques that have gained popularity over the past ten years have been used to detect malaria, from simple artificial neural networks and decision trees to random tree classifiers and support vector machine. But in a very small number of studies, classification methods have been created expressly for cell differentiation or parasite identification. The interaction of segmentation, features, and classification is where much of the domain knowledge pertaining to malaria is found. The assessment of the performance of the reported system can be quite difficult. The devices' performance was assessed using blood slides with widely varied settings for image collection and slide preparation. to make it possible to comment on the system's overall performance. There is currently no modest or big publicly accessible image benchmark collection that might be used to compare systems fairly. Because of this, even though many publications describe having relatively excellent performance, in our survey article we would rather not compare these metrics.

The runtime efficiency and accuracy of the processing pipeline may be shown to be in trade-off with one another. A technique's computational complexity often rises along with its accuracy. For cell segmentation, for instance, complex level-set techniques outperform Otsu thresholding, albeit at the cost of a longer runtime. The efficiency of the system can also be impacted by feature computation. In order to decrease feature dimensionality and eliminate non-discriminatory traits, some publications use feature selection techniques. This can increase accuracy and productivity. Finally, the employed classification architecture affects how quickly cells may be classified. For instance, a support vector machine's classification process is substantially quicker than a deep neural network. Even though many publications do not provide runtimes for their systems, we believe that, with some implementation optimization, the

majority of the listed systems would complete their tasks far more quickly than a microscopist, if not by a factor of ten [36,37].

Deep learning, the latest machine learning technique, has already shown promising results in many fields other than medicine. The popular multilayer neural network classifiers learned by back-propagation can be seen as an extension of deep learning but with many more layers. In conventional successions, many types of strata are also employed. Large training sets are often necessary for deep learning. Due to the difficulty of obtaining annotated training pictures due to the need for specialist knowledge and privacy considerations, deep learning is utilized by medical applications. After using a traditional level-set cell segmentation method, Liang et al.'s [38] are the first to use deep learning to diagnose malaria. They employ a convolutional neural network to distinguish between uninfected and infected cells and work on thin blood smears. Images of segmented red blood provide an excellent application for deep learning.

A major benefit of deep learning is considered to be that it does not require the creation of hand-crafted features, as other authors who have used deep learning to segment cells include Bibin et al.,[39] who utilized deep belief networks, Dong et al.,[40,41] and Gopakumar et al.,[37] who worked on convolutional neural networks, and most recently Hung et al.,[42] who employed a faster region-based convolutional neural network by providing an end-to-end framework. As deep learning is now a dominant approach in machine learning, we may anticipate a large number of new articles on cell staging, cell classification, cell segmentation, and many related issues concerned with automated malaria diagnosis.

3 DATASET

A total of 27,558 pictures were utilized in this study, with an exact rate of photos of uninfected and parasite cell types. The thin blood slide photos used in the Malaria Screener research project are the source of these photographs. It was researchers from the “National Library of Medicine's Lister Hill National Center for Biomedical Communications (LHNCBC)” that utilized an Android smartphone coupled to a standard light microscope to capture these photos. At “Chittagong Medical College Hospital in Bangladesh”, 50 healthy patients and 50 people who had been infected with malaria were imaged with Giemsa-stained thin blood smear slides. Photos of slides were taken using a smartphone's built-in camera, which were then labeled by a slide reader at the “Mahidol-Oxford Tropical Medicine Research Unit” based in Thailand. The “National Library of Medicine” has the de-identified images and comments. Figure 1 displays photos of parasite and uninfected cells.

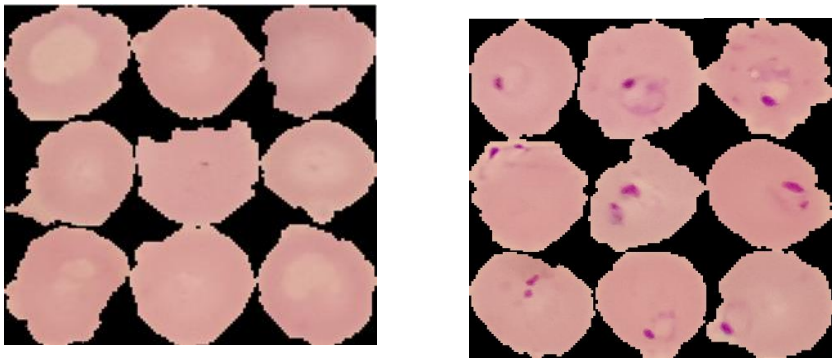

Figure 1: Uninfected and Infected Malaria cells

4 METHODOLOGY

In this section, an overview of our approach is presented, in which we have used pre-trained transfer learning models to detect malaria parasite cells.

4.1 Transfer Learning

Machine learning has been widely and effectively applied in a variety of applications where patterns from previous data (training data) may be retrieved to predict future events [43]. Traditional machine learning makes use of training and testing datasets that share the same data distribution and feature space. The results of a predictive learner might be affected if the distribution of data between training and testing changes. Training data that matches the test data's feature space and expected data distribution characteristics might be difficult to get in certain situations. That's why we need an expert in the target domain to come from a similar source domain. It's for this reason that we do things like this in the classroom [44].

This kind of learning is called "transfer learning," and it entails utilizing a model that you've already mastered. Basic transfer learning concepts are shown in Figure 2. Pre-trained models are essential since they are more complex and more accurate since they have been trained from a huge quantity of source data, namely “ImageNet”, and then "transfer" the learned knowledge to a relatively basic job (in this case, classifying uninfected from parasitized) with a small amount of data compared to the ImageNet dataset [45, 46].

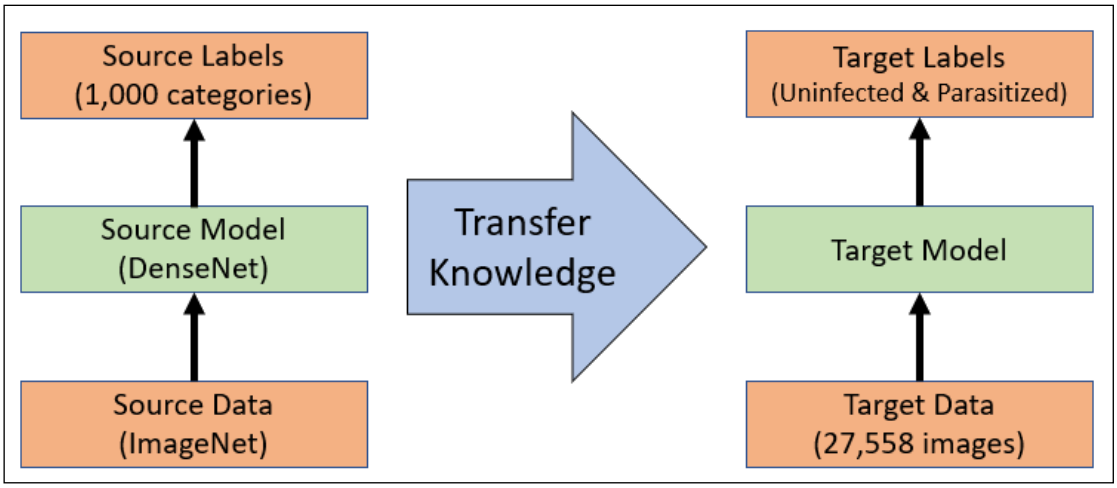

Figure 2: Transfer Learning Concept

A. DenseNet-121

When using a typical feed-forward convolutional neural network (CNN), the results of one layer are fed into the next one, except for the first (which receives input). Direct links between one layer and the next may be found for all "L" layers. There are certain drawbacks to this, though. For example, the "vanishing gradient" issue emerges when the number of layers in a CNN becomes larger. This means that the network's ability to train effectively is diminished as the channel for information between the input and the output layers expands, since some pieces of information may 'vanish' or be lost. By changing the typical CNN design and reducing the connecting pattern across layers, dense networks alleviate this issue. Each layer in a DenseNet architecture is connected to every other layer through direct connections, As a result, the name "Densely Connected Convolutional Network" emerged to describe this kind of neural network. Only two direct connections are available for each stratum.

With 120 convolutions and four average pools, DenseNet-121 is able to take use of characteristics retrieved earlier in the process. Due to the numerous duplicate features that the layers in the second and third dense blocks produce, they provide the least weight to the output of the transition layers. There may still be more high-level features created deeper within a model even when the weights of the whole dense block are employed by the final layers, since there appears to be a larger concentration of final feature maps in trials [47].

B. DenseNet-169

With The DenseNet family of image classification models includes the DenseNet-169 model. Densenet-121 and Densenet-169 models vary mostly in size and accuracy. When comparing the two, the densenet-169 is around 55MB larger, whereas the densenet-121 is just about 31MB.

DenseNet-169s CNN structure contains a dense block which has [6, 12, 32, 32] layers where the input feature maps of each previous sub-block are concatenated and then utilized as the input feature map of a specific sub-block. This extensive connection aids in the resolution of vanishing gradient issues and the reduction of parameter numbers [48].

C. DenseNet-201

The DenseNet family of image classification models includes the densenet-201 model as well. The densenet-201 model is bigger, at over 77MB, than the densenet-121 model, which is at around 31MB. Since the DenseNet-201 uses condensed networks, it allows for quick training and incredibly parametrically efficient models. In the next layer, this provides more options and improves performance. On a variety of datasets, such as ImageNet and CIFAR-100, DenseNet201 has performed very well. Direct connections from all previous levels to all subsequent layers are included in the DenseNet201 model to increase connectivity [49].

D. Xception

In 2017, Xception was developed, which was also known as Extreme Inception, a version belonging to the Inception family, which was developed by Chollet [50] at Google. The architecture of Xception is based on the concept of the Inception module [51], with modifications such as adding several convolution layers, depth-wise separable convolutions, inception modules, and residual connections to enhance the CNN performance. The results from Xception show performance improvments compared to ResNet, VGGNet, and InceptionV3 [52].

E. VGG16

VGG16 was developed by “A. Zisserman and K. Simonyan” from Oxford University in the publication titled "Very Deep Convolutional Networks for Large-Scale Image Recognition" in 2012. Using the ImageNet dataset, which comprises over 14 million pictures and 1000 classes, the model achieved a top-five test accuracy of 92.7 percent. VGG16 made improvements by replacing AlexNet’s large kernel-sized filters with several 3x3 kernel-sized filters in sequence. VGG16 was set to train for weeks using GPUs like NVIDIA Titan Black [53].

F. VGG19

VGG19 is a 19-layer variant of the VGG model (16 convolution layers, 3 Fully connected layer, 5 MaxPool layers and 1 SoftMax layer). VGG 19 has 19.6 billion floating point operations (FLOPs). The Visual Geometry Group at the University of Oxford created VGG19. VGG19 is also trained on the ImagNet dataset as a part of the (ILSVTC) challenge for 1000-class classification task. The network takes input as (224, 244, 3) RBG images [54].

G. Inception-V3

Inception-V3 is another CNN architecture with very good performance when it comes to object recognition. This model consists of three parts: the block of basic convolution, enhanced Inception module, and the classifier. In Inception-V3 the convolutional alternation with max-pooling layers occurs in the basic convolutional block which is used for feature extraction. Inception-V3 is an improved model from the original Inception module in which multi-scale convolutions are carried out in parallel and the results of the convolution of each branch are concatenated. Therefore, as a result of using the auxiliary classifiers, training results are more stable, which yields a better gradient convergence. At the same time, vanishing gradients the problem of overfitting are avoided [55].

H. InceptionResNetV2

InceptionResNetV2 is based on Inception-V3 and Microsoft's ResNet, the network is 164 with the ability to classify images since it is also trained on the image net dataset, therefor the network has learned a very rich representation through learning on the ImageNet dataset, the input size of the network is the size of 299-by-299 with an output list of the predicted probabilities of the class. In this network, the multiple-sized convolutional filters and the Inception-Resnet block are combined with the residual connections. The use of residual connections is not limited to the avoidance of the degradation problem that the deep structures might cause, but also to reduce the time of training [56].

I. MobileNet

MobileNet is a lightweight model that contains 4,253,864 parameters and accepts 224x224x3 images as input. and make use of a depth wise separable convolution block to extract features instead of the standard convolutional block. Depth wise convolution for each channel only uses 1 filter during convolution while the output of depth-wise convolution is merged by pointwise convolution. Therefore, in this network, depth-

wise convolution is applied to extract features from the images, and combining these features is accomplished through pointwise convolution [57].

J. MobileNetV2

It is a CNN model that has been enhanced from the original MobileNet model and has very good performance on mobile devices. This network is founded on the concept of a residual structure, in which the residual link is located in the midst of the bottleneck layers. As a source of non-linearity, the middle expansion layer makes use of lightweight convolutions that are depth-wise. Therefore, the MobileNetv2 architecture consists of an initially fully convolution layer containing 32 filters succeeded by 19 residual bottleneck layers [58].

5 EXPERIMENTS AND RESULTS

5.1 Performance Metrices

In order to measure real and predicted classes accuracy, precision, recall, and F1 score are used, which have been represented in Eqs. (1) - (4), respectively, as each performance metric's mathematical notation is provided below:

$$Accuracy = TP + TN\,TP + FN + FP + TN \tag{1}$$

$$Precision = TP\,TP + FP \tag{2}$$

$$Recal = TP\,TP + FN \tag{3}$$

$$F1 = 2 \times Precision \times Recall\,Precision + Recall \tag{4}$$

As "TP" stands for true positive, "TN" for true negative, "FP" for false positive, and "FN" for false negative.

5.2 Experiments

In this study, all of the tests were run on the Google Colab environment (1x Tesla K80 GPU). We used an Acer Aspire personal computer to interact with this environment. The number of epochs each model is trained on is 30, with a batch size of 32 and a learning rate of 0.001. The comparative findings for all the models are presented in Table X. It is clearly observed that DenseNet-201 has a slight edge over the other model's performance by achieving the highest scores in both Accuracy and F1-Score with 0.9339 and 0.9321, respectively. Also, DenseNet-169 has achieved the highest score on the Precision metric with 0.9597, and Densenet-121 performed the best in the Recall metrics with 0.9490. It's possible that this is because DenseNet models have the deepest neural structure, allowing them to map more complex patterns. MobileNet-V2 model has also performed very well, with an accuracy of 0.9302 and very high scores on the other metrices.

VGG16 and VGG19 have also achieved a good result by having 0.9277 and 0.9118 as their accuracies. While the MobileNetV1 model has achieved the lowest scores on accuracy, precision and F1 score with having 0.8732, 0.8298 and 0.8806. And the lowest score in the Recall category was achieved by the Xception model with 0.8282.

Table 1 Performance Comparison of Transfer Learning Models

Models	Accuracy	Precision	Recall	F1 Score
DenseNet-121	0.9262	0.9072	**0.9490**	0.9276
DenseNet-169	0.9299	**0.9597**	0.8971	0.9273
DenseNet-201	**0.9339**	0.9549	0.9104	**0.9321**
InceptionV3	0.8870	0.9284	0.8379	0.8808
Inception-ResNetV2	0.9262	0.9291	0.9223	0.9257
MobileNetV1	0.8732	0.8298	0.9381	0.8806
MobileNetV2	0.9302	0.9461	0.9119	0.9287
VGG16	0.9277	0.9355	0.9184	0.9269
VGG19	0.9118	0.9458	0.8731	0.9080
Xception	0.8923	0.9493	0.8282	0.8846

6 CONCLUSION

In this paper, we presented ten transfer learning models. We demonstrated that these models could be used to effectively tackle the identification of parasites from uninfected cells from red blood cell images. After evaluating these transfer learning models, we discovered that they could show competitive performance compared to each other. These models were tested on an image dataset. In the experiments, DenseNet-201 achieved the highest accuracy and F1 score, with DenseNet-169 and DenseNet-121 performing the best with Precision and Recall, respectively. While MobileNetV1 had the lowest precision and F1 score, The Xception model also performed the lowest in the Recall metric.

REFERENCES

1. "Fact sheet about malaria," World Health Organization, 26-Jul-2022. [Online]. Available: https://www.who.int/en/news-room/fact-sheets/detail/malaria.
2. M. T. Makler, C. J. Palmer, A. L. J. A. o. t. m. Ager, and parasitology, *A review of practical techniques for the diagnosis of malaria,* vol. 92, no. 4, 1998: p. 419-434.
3. J. Vink *et al.*, *An automatic vision-based malaria diagnosis system,* vol. 250, no. 3, 2013: p. 166-178.
4. Wongsrichanalai, Chansuda, et al. *A review of malaria diagnostic tools: microscopy and rapid diagnostic test (RDT).* Defining and Defeating the Intolerable Burden of Malaria III: Progress and Perspectives: Supplement to Volume 77 (6) of American Journal of Tropical Medicine and Hygiene, 2007.
5. S. M. Parsel *et al.*, *Malaria over-diagnosis in Cameroon: diagnostic accuracy of Fluorescence and Staining Technologies (FAST) Malaria Stain and LED microscopy versus Giemsa and bright field microscopy validated by polymerase chain reaction,* vol. 6, no. 1, 2017: p. 1-9.
6. G. Shute and T. J. B. o. t. W. H. O. Sodeman, *Identification of malaria parasites by fluorescence microscopy and acridine orange staining,* vol. 48, no. 5, 1973: p. 591.
7. I. Suwalka, A. Sanadhya, A. Mathur, and M. S. Chouhan, *Identify malaria parasite using pattern recognition technique, in 2012 International Conference on Computing, Communication and Applications*, 2012. IEEE.
8. J. Soni, N. Mishra, C. J. I. J. o. A. i. E. Kamargaonkar, and Technology, *Automatic differentiation between RBC and malarial parasites based ON morphology with first order features using image processing,* vol. 1, no. 5, 2011: p. 290.

9. C. W. Pirnstill and G. L. J. S. r. Coté, *Malaria diagnosis using a mobile phone polarized microscope,* vol. 5, no. 1, 2015: p. 1-13.
10. D. L. Omucheni, K. A. Kaduki, W. D. Bulimo, and H. K. J. M. j. Angeyo, *Application of principal component analysis to multispectral-multimodal optical image analysis for malaria diagnostics,* vol. 13, no. 1, 2014: p. 1-11.
11. D. Yang *et al.*, *A portable image-based cytometer for rapid malaria detection and quantification,* vol. 12, no. 6, 2017: p. e0179161.
12. S. A. Lee, R. Leitao, G. Zheng, S. Yang, A. Rodriguez, and C. J. P. o. Yang, *Color capable sub-pixel resolving optofluidic microscope and its application to blood cell imaging for malaria diagnosis,* vol. 6, no. 10, 2011: p. e26127.
13. Z. Zhang *et al.*, *Image classification of unlabeled malaria parasites in red blood cells,* in 2016 38th *Annual International Conference of the IEEE Engineering in Medicine and Biology Society (EMBC)*. 2016. IEEE,.
14. S. Bhowmick, D. K. Das, A. K. Maiti, and C. J. M. Chakraborty, *Structural and textural classification of erythrocytes in anaemic cases: a scanning electron microscopic study,* vol. 44, 2013: p. 384-394,.
15. F. Ajala, O. Fenwa, and M. J. I. J. A. I. S. Aku, *Comparative analysis of different types of malaria diseases using first order features,* vol. 8, 2015: p. 20-6.
16. D. K. Das, M. Ghosh, M. Pal, A. K. Maiti, and C. J. M. Chakraborty, *Machine learning approach for automated screening of malaria parasite using light microscopic images*, vol. 45, 2013: p. 97-106.
17. C. Ma, P. Harrison, L. Wang, and R. L. J. M. j. Coppel, *Automated estimation of parasitaemia of Plasmodium yoelii-infected mice by digital image analysis of Giemsa-stained thin blood smears,* vol. 9, no. 1, 2010: p. 1-9.
18. M. I. J. I. J. I. P. Razzak, *Malarial parasite classification using recurrent neural network,* vol. 9, 2015: p. 69.
19. N. Ahirwar, S. Pattnaik, B. J. I. J. o. I. T. Acharya, and K. Management, *Advanced image analysis based system for automatic detection and classification of malarial parasite in blood images,* vol. 5, no. 1, 2012: p. 59-64.
20. S. Savkare and S. J. P. T. Narote, *Automatic system for classification of erythrocytes infected with malaria and identification of parasite's life stage*, vol. 6, 2012: p. 405-410.

21. G. Díaz, F. Gonzalez, and E. Romero, *Infected cell identification in thin blood images based on color pixel classification: comparison and analysis,* in *Iberoamerican Congress on Pattern Recognition*. 2007. Springer.
22. M. Brückner, K. Becker, J. Popp, and T. J. A. c. a. Frosch, *Fiber array based hyperspectral Raman imaging for chemical selective analysis of malaria-infected red blood cells,* vol. 894, 2015: p. 76-84.
23. A. J. C. P. S. U. Von Mühlen, San Luis Obispo, *Computer image analysis of malarial Plasmodium vivax in human red blood cells*, 2004.
24. L. Malihi, K. Ansari-Asl, and A. Behbahani, *Malaria parasite detection in giemsa-stained blood cell images, in 2013 8th Iranian conference on machine vision and image processing (MVIP).* 2013. IEEE.
25. N. E. Ross, C. J. Pritchard, D. M. Rubin, A. G. J. M. Duse, B. Engineering, and Computing, *Automated image processing method for the diagnosis and classification of malaria on thin blood smears,* vol. 44, no. 5, 2006: p. 427-436.
26. J. Vermillion, E. Wilson, and R. J. H. Smith, *Traumatic diaphragmatic hernia presenting as a tension fecopneumothorax,* vol. 5, no. 3, 2001: p. 158-160.
27. N. Abbas and J. Andersson, *Architectural reasoning for dynamic software product lines, in Proceedings of the 17th International Software Product Line Conference Co-located Workshops.* 2013.
28. S. W. Sio *et al.*, *MalariaCount: an image analysis-based program for the accurate determination of parasitemia*, vol. 68, no. 1, 2007: pp. 11-18.
29. N. Abbas *et al.*, *Machine aided malaria parasitemia detection in Giemsa-stained thin blood smears,* vol. 29, no. 3, 2018: p. 803-818.
30. N.-T. Nguyen, A.-D. Duong, and H.-Q. Vu, *A new method for splitting clumped cells in red blood images, in Second International Conference on Knowledge and Systems Engineering*. 2010. IEEE,.
31. S. S. Devi, A. Roy, M. Sharma, and R. Laskar, *KNN classification based erythrocyte separation in microscopic images of thin blood smear,* in *2016 2nd International Conference on Computational Intelligence and Networks (CINE)*. 2016. IEEE.

32. S. K. Kumarasamy, S. Ong, K. S. J. M. V. Tan, and Applications, *Robust contour reconstruction of red blood cells and parasites in the automated identification of the stages of malarial infection,* vol. 22, no. 3, 2011: p. 461-469.
33. A. S. Abdul-Nasir, M. Y. Mashor, and Z. J. W. T. B. B. Mohamed, *Colour image segmentation approach for detection of malaria parasites using various colour models and k-means clustering,* vol. 10, no. 1, 2013: p. 41-55.
34. D. M. Memeu, *A rapid malaria diagnostic method based on automatic detection and classification of plasmodium parasites in stained thin blood smear images,* University of Nairobi. 2014.
35. A. K. Subhamoy Mandal, J Chatterjee, M Manjunatha, Ajoy K Ray, *Segmentation of blood smear images using normalized cuts for detection of malarial parasites,* presented at *the Annual IEEE India Conference* (INDICON).2010. IEEE.
36. S. Kaewkamnerd, C. Uthaipibull, A. Intarapanich, M. Pannarut, S. Chaotheing, and S. Tongsima, *An automatic device for detection and classification of malaria parasite species in thick blood film, BMC Bioinformatics,* vol. 13, no. 17, 2012: p. S18.
37. G. P. Gopakumar, M. Swetha, G. Sai Siva, and G. R. K. Sai Subrahmanyam, *Convolutional neural network-based malaria diagnosis from focus stack of blood smear images acquired using custom-built slide scanner,* vol. 11, no. 3, 2018.
38. Z. Liang *et al.*, *CNN-based image analysis for malaria diagnosis, in IEEE international conference on bioinformatics and biomedicine (BIBM)*. 2016. IEEE.
39. D. Bibin, M. S. Nair, and P. J. I. A. Punitha, *Malaria parasite detection from peripheral blood smear images using deep belief networks,* vol. 5, 2017: p. 9099-9108.
40. Y. Dong *et al.*, *Evaluations of deep convolutional neural networks for automatic identification of malaria infected cells,* in *2017 IEEE EMBS international conference on biomedical & health informatics (BHI)*. 2017. IEEE.
41. Y. Dong, Y. Liu, D. Lu, F. Zheng, P. Fang, and H. J. S. S. S. Zhang, *Unpredictable adsorption and visible light induced decolorization of nano rutile for the treatment of crystal violet,* vol. 66, 2017: p. 1-6.
42. J. Hung and A. Carpenter, *Applying faster R-CNN for object detection on malaria images,* in *Proceedings of the IEEE conference on computer vision and pattern recognition workshops*. 2017. IEEE.

43. A. H. Awlla, B. T. Muhammed, S. H. Murad, and S. N. Ahmad, *Prediction of covid-19 mortality in Iraq-kurdistan by using machine learning*, UHD Journal of Science and Technology, vol. 5, no. 1, 2021: p. 66–70.
44. K. Weiss, T. M. Khoshgoftaar, and D. J. J. o. B. d. Wang, *A survey of transfer learning*, vol. 3, no. 1, 2016: p. 1-40.
45. K.-j. Xia, H.-s. Yin, and J.-q. J. C. C. Wang, *A novel improved deep convolutional neural network model for medical image fusion*, vol. 22, no. 1, 2019: p. 1515-1527.
46. K.-j. Xia, H.-s. Yin, and Y.-d. J. J. o. m. s. Zhang, *Deep semantic segmentation of kidney and space-occupying lesion area based on SCNN and ResNet models combined with SIFT-flow algorithm*, vol. 43, no. 1, 2019: p. 1-12.
47. G. Huang, Z. Liu, L. Van Der Maaten, and K. Q. Weinberger, *Densely connected convolutional networks*, in *Proceedings of the IEEE conference on computer vision and pattern recognition*. 2017. IEEE.
48. F. Chollet, *Xception: Deep learning with depthwise separable convolutions*, in *Proceedings of the IEEE conference on computer vision and pattern recognition*, 2017. IEEE.
49. C. Szegedy *et al.*, *Going deeper with convolutions*, in *Proceedings of the IEEE conference on computer vision and pattern recognition*, 2015: p. 1-9.
50. C. Szegedy, V. Vanhoucke, S. Ioffe, J. Shlens, and Z. Wojna, *Rethinking the inception architecture for computer vision*, in *Proceedings of the IEEE conference on computer vision and pattern recognition*, 2016. IEEE.
51. X. Zhang, J. Zou, K. He, J. J. I. t. o. p. a. Sun, and m. intelligence, *Accelerating very deep convolutional networks for classification and detection*, vol. 38, no. 10, 2015: p. 1943-1955.
52. *Fact sheet about malaria*, World Health Organization, 26-Jul-2022. [Online]. Available: https://www.who.int/en/news-room/fact-sheets/detail/malaria.
53. S. S. Han *et al.*, *Deep neural networks show an equivalent and often superior performance to dermatologists in onychomycosis diagnosis: Automatic construction of onychomycosis datasets by region-based convolutional deep neural network*, vol. 13, no. 1, 2018: p. e0191493.
54. C. Lin, L. Li, W. Luo, K. C. Wang, and J. J. P. P. T. E. Guo, *Transfer learning based traffic sign recognition using inception-v3 model*, vol. 47, no. 3, 2019: p. 242-250.

55. Z. Elhamraoui, *INCEPTIONRESNETV2 simple introduction*, Medium, 16-May-2020. [Online]. Available:https://medium.com/@zahraelhamraoui1997/inceptionresnetv2-simple-introduction-9a2000edcdb6.
56. T. Ghosh *et al.*, *Bangla handwritten character recognition using MobileNet V1 architecture*, vol. 9, no. 6, 2020: p. 2547-2554.
57. Pan, Haihong, et al. *A new image recognition and classification method combining transfer learning algorithm and mobilenet model for welding defects. IEEE Access*, 2020: p.119951-119960.
58. M. Sandler, A. Howard, M. Zhu, A. Zhmoginov, and L.-C. Chen, *Mobilenetv2: Inverted residuals and linear bottlenecks*, in *Proceedings of the IEEE conference on computer vision and pattern recognition*. 2018. IEEE.